J Therm Anal Calorim (2010) 102:837–849
DOI 10.1007/s10973-010-0831-8

Study of experimental and theoretical procedures when using thermogravimetric analysis to determine kinetic parameters of carbon black oxidation

N. Zouaoui · J. F. Brilhac · F. Mechati · M. Jeguirim · B. Djellouli · P. Gilot

Received: 25 November 2009 / Accepted: 20 April 2010 / Published online: 13 May 2010

Abstract Combustion of carbon black (CB) in the crucible of a thermobalance is controlled by both carbon reactivity and oxygen transport from the oxidizing flux to the surface of the bed and within the porous bed. The kinetic constant of combustion has been determined using a fixed-bed reactor in which CB combustion is mainly under kinetic control. Then, modelling of oxygen transport in the thermobalance allowed determining the oxygen diffusivity within the CB pile. Fickian diffusion is a good approximate value of the diffusion coefficient for modelling of internal oxygen transport. The effects of the initial sample mass and of the sample containment on the initial combustion rate have been investigated. The effectiveness factor of the bed was calculated for different experimental conditions. Advices to correctly extract a kinetic constant from thermogravimetric experiments are given. According to the required precision, an experimental procedure is proposed. Limitations to oxygen transport within the bed may be ignored. They can be minimized by the use of an inert material to remove the stagnant atmosphere between the surface of the bed and the mouth of the crucible. It appears mandatory to account for oxygen transport limitations within the CB pile. It can be assumed that the sample temperature (not known) during reaction is the regulation temperature. Thermal effects are also minimized by use of the inert material. A 30–50 mg sample mass seems to be optimal for determination of the kinetic parameters.

Keywords Thermogravimetry · Kinetics of combustion · Mass transfer · Reaction engineering · Porous media · Carbon black

List of symbols

c	Concentration of gas, mol m^{-3}
D_{O_2}	Diffusivity of oxygen, m^2 s^{-1}
e	Thickness of the bed of CB, m
k	Kinetic constant used in thermogravimetry, s^{-1}
k^{FB}	Kinetic constant obtained by fixed-bed experiments, s^{-1}
k_1	Kinetic constant obtained from thermogravimetric experiments and use of procedure 1 to extract the constant, s^{-1}
k_2	Kinetic constant obtained from thermogravimetric experiments and use of procedure 2 to extract the constant, s^{-1}
k_3	Kinetic constant obtained from thermogravimetric experiments and use of procedure 3 to extract the constant, s^{-1}
k_4	Kinetic constant obtained from thermogravimetric experiments and use of procedure 4 to extract the constant, s^{-1}
f	Stoichiometric coefficient, $mol_{O_2} mol_C^{-1}$
m_0	Initial sample mass, kg
M_c	Molar mass of carbon, kg mol^{-1}
R_1	Ratio k_1/k^{FB} calculated at the sample temperature
R_2	Ratio k_2/k^{FB} calculated at the regulation temperature

N. Zouaoui · J. F. Brilhac · F. Mechati · M. Jeguirim · P. Gilot (✉)
Laboratoire Gestion des Risques et Environnement, Université de Haute Alsace, 25 Rue de Chemnitz, 68200 Mulhouse, France
e-mail: patrick.gilot@uha.fr

N. Zouaoui · B. Djellouli
Laboratoire Génie des Procédés Chimiques, Université Ferhat Abbas, Sétif, Algeria

R_3	Ratio k_3/k^{FB} calculated at the regulation temperature
R_4	Ratio k_4/k^{FB} calculated at the regulation temperature
R_C	Combustion rate of CB measured by thermogravimetry, kg s^{-1}
R_c^{FB}	Combustion rate of CB measured with the fixed bed, kg s^{-1}
$(R_C)_{max}$	Maximum combustion rate for $X = X_s$ within the bed, kg s^{-1}
$((R_C)_{max})_{in}$	Maximum combustion rate for $X = X_{in}$ within the bed, kg s^{-1}
S	Area of the section of the crucible, m^2
T	Bed temperature, K
T_R	Regulation temperature, K
X	Molar fraction of oxygen
X_{in}	Inlet molar fraction of oxygen
X_S	Molar fraction of oxygen at the surface of the bed
z	Coordinate along the bed thickness, m

Greek letters

β	Reaction order
ε	Total porosity of the bed
η	Effectiveness factor of the bed
ρ	True graphite density, kg m^{-3}
ρ_{bed}	Bed density, kg m^{-3}
τ	Tortuosity of the bed

Introduction

Thermogravimetric analysis is a very useful technique to measure the combustion rate of a solid under well defined conditions such as temperature and oxygen concentration [1–6]. The accuracy of the weight loss measurements is very high. However, the combustion rate obtained from the weight loss plotted versus time depends on the arrangement of the solid and the crucible which affects the access of oxygen to the solid surface [7, 8]. This makes more difficult to extract fundamental kinetic information from the experimental results. To derive an intrinsic kinetic constant becomes even more difficult when a very porous medium in which oxygen penetrates is deposited within the crucible. Oxygen diffusion, both external to reach the sample surface and internal inside the porous medium, governs, together with kinetics, the rate of the solid combustion [9–11]. When the solid material is carbon black (CB), the problem becomes more complex since the solid reactivity changes during the course of oxidation, due to structure modifications. Specific surface area of CB is known to increase during combustion, in relation with the increase of porosity [12–14]. However, only a part of this surface, the active surface area, is expected to play a role during oxidation [15]. Nguyen et al. and Jung et al., showed the decrease of the size of the spherules during combustion [16, 17]. The structural change of CB during oxidation affects oxygen transport within the porous medium, contributing also by this way to the change of the oxidation rate. Very often, a mean combustion rate is extracted from the quasi linear part of the thermogram.

A fixed-bed reactor with oxygen flowing through the porous bed of CB is another technique currently used to study combustion. The instantaneous combustion rate is calculated from CO and CO_2 emissions and the accuracy is less than for the thermogravimetric technique. Combustion is, a priori, mainly governed by kinetics since the fixed-bed operates as a differential reactor and oxygen diffusion is not expected to play a significant role.

The goal of this paper is to propose the best experimental and theoretical procedures to extract a kinetic constant from thermogravimetric experiments. It is important to well understand how oxidation of CB proceeds in the crucible of a thermobalance under different experimental conditions. This understanding allows giving indications for extracting intrinsic kinetic parameters. This procedure can apply to the study of the reactivity of diesel soot which has a structure very close to that of CB. The obtained kinetic parameters are used by researchers modelling the regeneration of particulate traps now installed in the exhaust lines of cars equipped with a diesel engine. There is a need of very reliable kinetic parameters to have a good prediction of the regeneration behaviour.

The objective of this paper is not to study the evolution of the CB structure during the course of combustion. Only few results regarding the change of CB structure are given. The original state of CB is taken and used to extract combustion parameters.

Experimental

The material involved in this study is commercial CB named Vulcan 6. The elemental composition is 95.3% C, 2.1% O, 0.7% H, 1% S, <0.3% N. The apparent density ρ_{bed} of the bed of CB is 360 kg m^{-3}. The bed of CB comprises particulates (mean diameter 25 μm) which are agglomerates of aggregates (diameter 100 nm) built with 32 nm spherules. Using the measured bed density and the true graphite density ($\rho = 2000$ kg m^{-3}), the total porosity of a CB sample is $\varepsilon = 1 - \frac{\rho_{bed}}{\rho} = 0.82$.

Thermogravimetric analysis was performed with a Setaram thermobalance. A scheme of the experimental system is represented in Fig. 1. First the reactor (13 mm of internal diameter) was purged under nitrogen (5 L h^{-1}) at room temperature during 1 h.

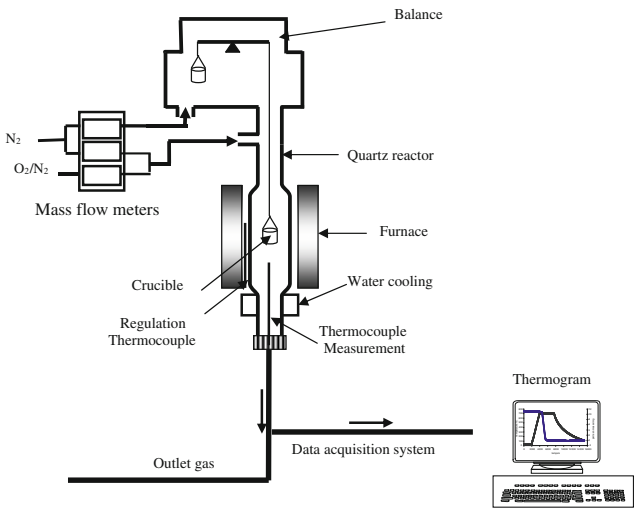

Fig. 1 Schematic diagram of the thermobalance

For combustion tests, an isothermal mode was applied. Samples of CB with initial masses ranging from 10 to 80 mg were submitted to a temperature ramp (20 °C min^{-1}) under nitrogen up to the desired temperature. This temperature was maintained constant during 30 min under the nitrogen flow. Then, the nitrogen flow was stopped and an oxidising flow containing 2 and 10% oxygen was admitted in the reactor. The gas flow rate was controlled by Brooks mass flow meters. For most of the experiments, the gas flow rate was kept constant at 3 L h^{-1} (standard conditions). The gas flow rate was only varied from 1 to 5 L h^{-1} to investigate its effect on the combustion rate.

The gas was supplied vertically above the crucible. Different crucibles (7 mm internal diameter and 6–12 mm height) were used. In some tests, a bed of inert material (silicium carbide) was deposited below the bed of CB to completely fill up the crucible and avoid the presence of a stagnant volume between the surface of the bed of CB and the mouth of the crucible.

The thickness of a 20 mg sample of CB was roughly 1.4 mm. For the 10 mg sample, particles just made a one to three particle layer covering the whole section of the bed of inert material. Then, for 10 mg of CB and below, it is better to consider individual particles rather than a bed.

A thermocouple located within the reactor 2 cm below the crucible measured the gas temperature and permitted the regulation of the temperature according to the temperature program.

The measured gas temperature may be different from the bed temperature which controls the combustion rate. For that reason, another apparatus, called special temperature measurement device, was designed to obtain only the bed temperature during reaction. The reaction rate was not determined with this system. A crucible normally used for thermogravimetry was suspended in the isothermal zone of a cylindrical reactor (16 mm of internal diameter, different from the reactor of the thermobalance) placed within a cylindrical oven. The oven temperature was regulated by a thermocouple located outside the reactor. Two thermocouples measured gas temperatures 1 cm below and 1 cm above the crucible. A third one was located within the bed of CB to measure the solid temperature during combustion. In this temperature measurement device, the gas flow rate was adjusted to 5 L h^{-1} in order to get the same residence time of the gas within the reactor as during thermogravimetric experiments for which 3 L h^{-1} was normally used. The temperature program was the same as that used for thermogravimetric analysis. The reaction was expected to operate as it did with the thermobalance. We make the hypothesis that the measured bed temperature was the same as that prevailing in the bed in the test carried out under the same conditions with the thermobalance.

Combustion tests were also performed using a fixed-bed reactor. Combustion rates were calculated from measured CO and CO_2 emissions. Due to CO and CO_2 analyser's constraints, the gas flow rate was set to 70 L h^{-1}. With this gas flow rate, the response time of the CO and CO_2 analyser is roughly 12 s, including the time necessary for CO and CO_2 to come from the reactor inlet to the measurement cell. Reaction temperature was measured by a thermocouple located within the sample bed.

The specific surface area of the CB sample, before reaction and after different conversion levels, was measured by the BET procedure using a Micromeritics apparatus. The sample was degassed at 450 °C. The change of the BET surface area was investigated versus conversion after combustion in the fixed-bed reactor, under two combustion rate conditions: 570 °C, 2% oxygen corresponding to low combustion rates and 620 °C, 10% oxygen corresponding to high combustion rates.

Results

For comparison, 50 mg of CB was submitted to 10% oxygen at 600 °C in a fixed-bed reactor and in a thermobalance. The combustion rate is plotted versus conversion in Fig. 2. The shapes of the curves are very comparable but the maximum combustion rate is roughly five times greater in the fixed-bed reactor. This proves that oxygen diffusion at least partly controls the rate of combustion in the thermobalance.

Fixed-bed experiments

All the performed experiments under different conditions returned a combustion curve with a maximum (see Fig. 2)

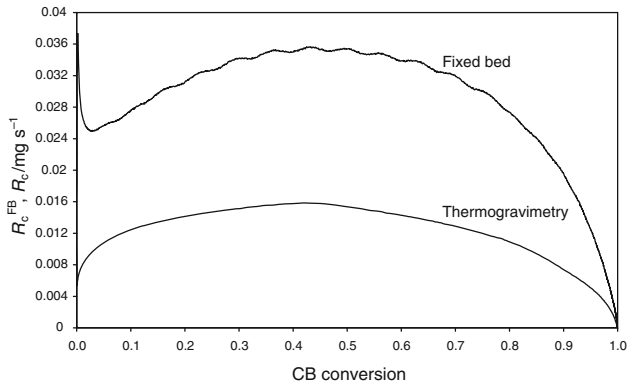

Fig. 2 Comparison between combustion rates versus burn off when a fixed-bed reactor or a thermobalance are used. Combustion of 50 mg of CB; 10% oxygen. Regulation temperature: 600 °C

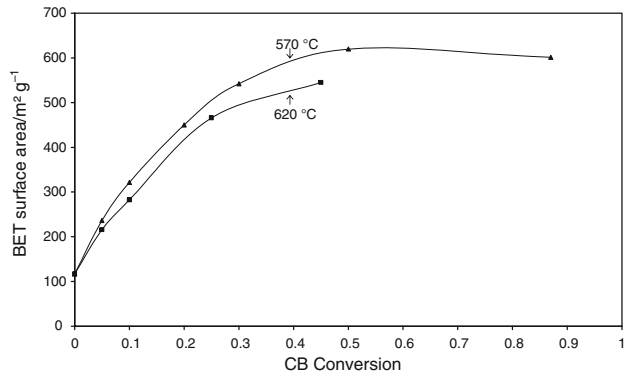

Fig. 3 Specific surface area versus burn off during combustion of 50 mg of CB under two different conditions in the fixed bed

at roughly 50% conversion. It was not detected a temperature increase within the CB bed during the course of combustion. To justify the existence of this maximum, the BET surface area is plotted versus conversion when combustion was performed under two different sets of conditions (see Fig. 3). The specific surface area of the original CB is 117 m^2 g^{-1}. If one considers that only the surface of non-porous spherules contributes to that BET surface, one obtains 94 m^2 g^{-1}. To reconcile these two specific surface areas, one must consider some initial porosity within the spherules. This means that during fixed-bed combustion, oxygen is transported through the bed by both convection through the porosity between spherules and diffusion through the internal porosity of spherules.

Under conditions for a high combustion rate, the specific surface area increases drastically with conversion during the first 30% conversion, still increases up to 620 m^2 g^{-1} at 52% conversion and then levels off up to the end of combustion. The specific surface area evolves in a comparable way for low combustion rates.

This increase of the specific surface area explains why the combustion rate increases up to roughly 50% conversion despite the CB consumption.

Above 50% burn off, the combustion rate is essentially governed by the instantaneous value of the sample mass.

At the beginning of combustion, after 12 s necessary for the analysers to detect CO and CO_2, there is a sharp decrease of the combustion rate lasting 800 s (560 °C, 2% oxygen, 100 mg) or 35 s (620 °C, 10% oxygen, 10 mg). The corresponding carbon conversion is 3 or 5%, respectively. This high initial combustion rate is due to reaction of very active sites for strong oxygen adsorption after the CB surface has been exposed to N_2 [14]. The specific surface area at the end of this period is roughly 220 m^2 g^{-1} (whatever the combustion conditions), proving a large development of porosity. The very initial rate (corresponding to time t equal to 0 taken at oxygen injection) is unknown, due to the response time of the analysers. In order to approximate the combustion rate of the initial material, one decided to consider the first reliable measured rate (noted R_c^{FB}) at time t equal to 15 s (the necessary time for the analyser to respond).

Using initial experimental combustion rates R_c^{FB} obtained for isothermal combustion of different sample masses of CB at different temperatures, and assuming that these rates are proportional to the initial sample mass, one obtains the kinetic constants k^{FB} from

$$R_C^{FB} = k^{FB} m_0 X^{\beta} \quad (1)$$

The value of β was found at 0.88.

The kinetic constant may be written in an Arrhenius form:

$$k^{FB} = 5.79 \times 10^5 \exp(-136200/RT) \quad (2)$$

Due to the difficulty to estimate the initial combustion rate, the relative uncertainty was assumed at roughly 15%. This value accounts for the presence of the initial peak (see for example Fig. 2). At time 15 s, chosen to record the combustion rate, this rate is somewhere between the maximum and the minimum generated by the peak, and depending on experimental conditions. The estimated value of 15% is determined by considering the rate domain situated between these two extrema.

This rate constant will be used further to characterize initial CB combustion. This kinetic constant is not an intrinsic one since it's affected by oxygen diffusion within spherules.

Thermogravimetric experiments

All the obtained thermograms present the same aspect. During the temperature ramp before introduction of the oxidising flux, a weight loss of roughly 2 mg was recorded,

and then a quasi linear weight loss was obtained under the temperature plateau until the end of combustion. The amount of ashes was not significant. When the oxidising flux was injected by opening of an electro-valve, a mechanical perturbation of the equilibrium made the mass measurement impossible during roughly 120 s. There is also a necessary delay of roughly 100 s for oxygen to reach its desired concentration at the level of the crucible. This means that the first reliable measurement point is situated 120 s after the injection time of the oxidising flux. At this point, the CB conversion is very low, it does not exceed 0.3% for example in the case of oxidation of 50 mg of CB at 600 °C. The "initial" combustion rate was arbitrarily taken at the end of the mechanical perturbation.

Effect of the presence of the stagnant volume between the surface of the CB bed and the mouth of the crucible

To reach the surface of the bed of CB, oxygen must diffuse from the oxidising flux admitted in the thermobalance to the mouth of the crucible and then to the surface of the bed of CB. In that case, no inert material was used.

Using always 50 mg of CB, three different crucibles were used to vary the depth d of the stagnant volume within the crucible. The regulation temperature was 600 °C and the gas flow rate 3 L h^{-1}. Combustion rates are presented on Fig. 4. The increase of d from 2 to 8 mm had a strong effect on the combustion rate which fell from 0.011 to 0.007 mg s^{-1} at its maximum. This is due to the decrease of the local oxygen concentration at the surface of the bed of CB.

Effect of the gas flow rate

Combustion of 50 mg of CB was carried out, using a regulation temperature of 600 °C for three different gas flow rates: 1, 3 and 5 L h^{-1}. There was no inert material. Combustion rates versus time are given in Fig. 5. The combustion rates were strongly affected when the gas flow rate was changed from 1 to 3 L h^{-1}. Only a small effect was detected between 3 and 5 L h^{-1}. This effect is caused by modifications of oxygen transport from the injected oxidising flow to the mouth of the crucible. Since the convective flow is deviated by the presence of the crucible, oxygen is mainly transported by diffusion.

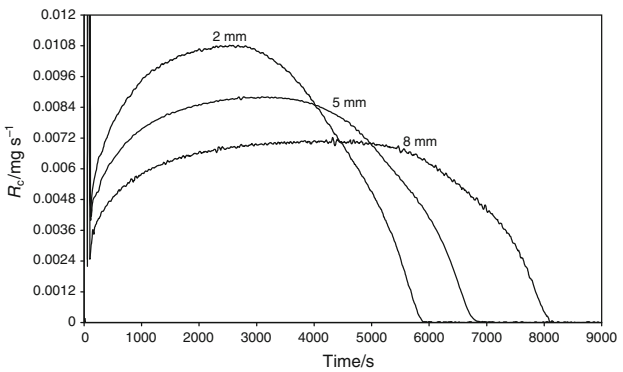

Fig. 4 Effect of the presence of the stagnant volume between the surface of the CB bed and the mouth of the crucible. Combustion of 50 mg of CB with three different distances between the surface of the bed and the mouth of the crucible. Regulation temperature: 600 °C; 2% oxygen

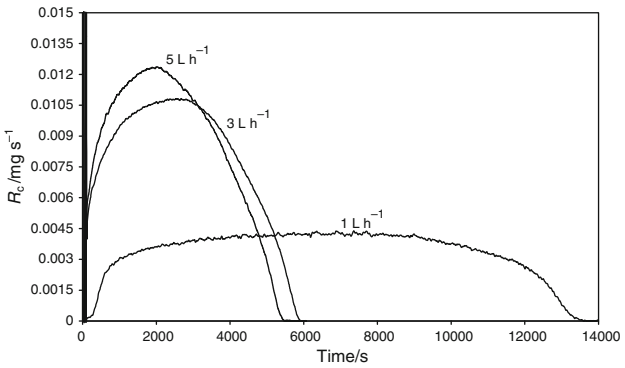

Fig. 5 Effect of the gas flow rate on the combustion rates of 50 mg of CB. Regulation temperature: 600 °C; 10% oxygen

Effect of the initial mass of the CB sample

For this study, to avoid the effect of the stagnant volume between the surface of the bed and the mouth of the crucible, the necessary mass of inert material was deposited in the bottom of the crucible in order to have the surface of CB levelling at the mouth of the crucible.

The repeatability of measurements has been investigated in the following conditions: 600 °C, 10% O_2. These tests showed how important is the filling of the crucible. When the soot surface is very flat and when the void volume of the crucible is exactly filled with CB, the dispersion of the measured combustion rates is less than 3%.

Combustion rates corresponding to combustion at 650 °C in 10% oxygen of different initial masses of *CB* ranging from 10 to 80 mg are given on Fig. 6. These conditions are favourable for a high combustion rate.

During the first 700 s of combustion, the combustion rates of the samples with masses equal or higher than 17.5 mg are identical. During the first 2200 s of combustion, the combustion rates of the 50 and 80 mg samples are also the same. The samples with initial masses smaller than 17.5 mg exhibit a combustion rate decreasing with the initial sample mass.

This behaviour is characteristic of heterogeneous combustion within the samples, controlled by both oxygen diffusion through the CB pile and kinetics. If combustion was occurring only at surface of the bed, the initial

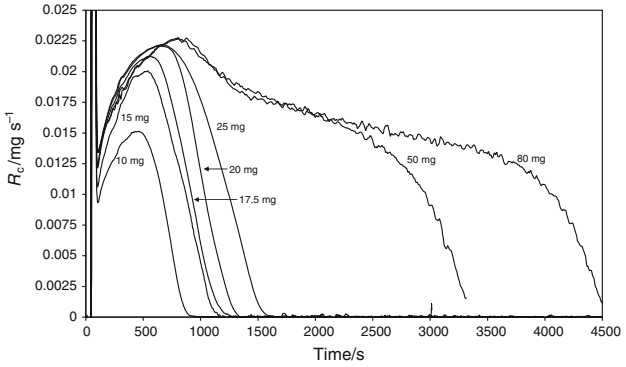

Fig. 6 Combustion rates corresponding to combustion of different sample masses of CB. Regulation temperature: 650 °C; 10% oxygen

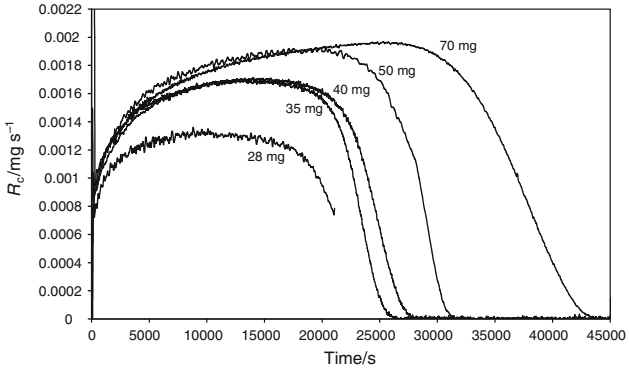

Fig. 8 Combustion rates corresponding to combustion of different sample masses of CB. Regulation temperature: 570 °C; 2% oxygen

combustion rates would be the same for all the samples and would be very close to the value obtained for the 10 mg sample since there is no bed for that mass. An oxygen concentration gradient establishes within the bed and the combustion rate is related to the oxygen mole fraction profile within the sample. Then, the fact that initial combustion rates obtained for masses in the range 80 to 17.5 mg are the same, proves that oxygen mole fraction profiles along the bed thickness are identical (or very close) for these samples. The oxygen mole fraction should fall to zero before the bottom of the bed and only a part of the bed should be burning (see Fig. 7a). During combustion, the specific area of CB increases, increasing first the combustion rate despite the CB consumption. Then a maximum is obtained due to CB consumption and the combustion rate starts to fall down. The combustion zone moves towards the bottom of the bed and when it reaches the bottom of the bed, the combustion rate of the bed drastically decreases.

For 15 and 10 mg samples, the whole sample should be burning, with an oxygen concentration decreasing with oxygen penetration, but still higher than zero at the bottom of the bed (see Fig. 7b). The mass of burning CB decreases with the thickness of the bed, explaining why the combustion rate decreases with the initial sample mass.

A critical sample mass noted m_0^* (between 15 and 17.5 mg) corresponds to the transition from a constant initial combustion rate to a decreasing one. For that particular mass, the oxygen mole fraction probably should fall to a value close to zero at the bottom of the bed.

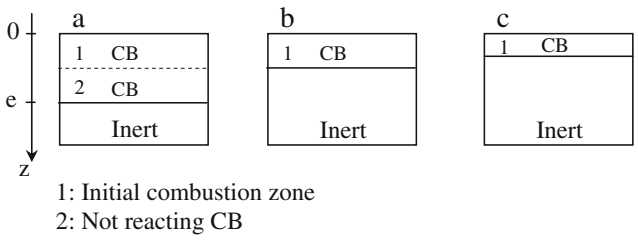

Fig. 7 Scheme showing the arrangement of *CB* and inert material and the initial combustion zone for different sample masses of CB. *a*: $m_0 > m_0^*$, *b*: $m_0 = m_0^*$, *c*: $m_0 < m_0^*$

Combustion rates of different sample masses ranging from 28 to 70 mg burning at 570 °C in 2% oxygen are given on Fig. 8. These conditions are favourable for a low combustion rate. The combustion rates during the first 80 min of combustion are almost superimposed for initial masses in the range 70–35 mg. As previously, a mixed combustion regime, controlled by both kinetics and diffusion, prevails with an oxygen concentration gradient within the CB bed. The difference with the previous case is that oxygen penetrates deeper within the bed, due to lower temperature and oxygen content. The critical sample mass, for which the oxygen concentration falls close to zero at the surface of the inert material, is close to 35 mg. For a mass smaller than 35 mg, the oxygen distribution depends on the CB bed thickness. Roughly, larger the thickness is, higher the combustion rate.

Intermediate combustion rates were obtained using a regulation temperature equal to 600 °C and an oxygen content of 10% (see Fig. 9). In that case, only combustion

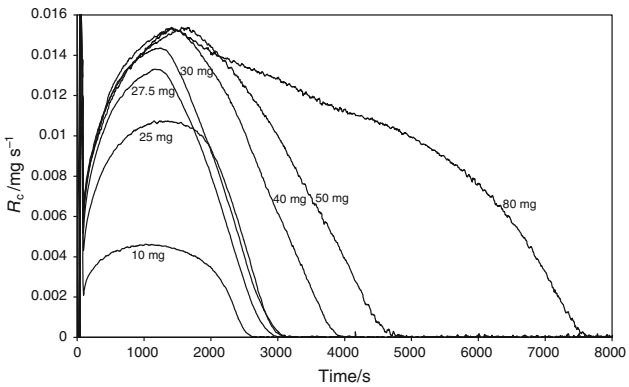

Fig. 9 Combustion rates corresponding to combustion different sample masses of CB. Regulation temperature: 600 °C; 10% oxygen

rates for the 30, 40, 50 and 80 mg samples are the same during roughly 1000 s of combustion. Combustion rates for the 27.5, 25 and 10 mg samples are lower whatever conversion. This means that the initial combustion zone is the same for the four larger sample masses until the point where the curves separate. At this point, the combustion zone corresponding to the 30 mg sample reaches the interface with the inert material and the combustion zone corresponding to the larger samples continues to expand. The combustion of the 10, 25 and 27.5 mg samples affects the whole bed and is very dependent on the sample mass. Under these experimental conditions, 30 mg may be chosen as the critical sample mass.

Another intermediate condition, regulation temperature of 570 °C associated to 10% oxygen gives a similar combustion mechanism. For this set of conditions, a critical sample mass of 35 mg was experimentally determined.

The sample temperatures during combustion were measured using the specific temperature measurement device previously presented. The maximum bed temperature increase during combustion was estimated. Due to the difficulty to place the thermocouple within the thin bed of CB, only an order of magnitude of this bed temperature increase was obtained. A reliable measurement was not possible for bed masses smaller than 40 mg. These temperatures are given in Table 1 for the different experimental situations. The maximum temperature increase was obtained when the combustion rate was close to its maximum and drastically decreased with the combustion rate, as expected. The maximum detected temperature increase was roughly 20 °C for a regulation temperature equal to 650 °C and a 80 or 50 mg sample under 10% oxygen at a gas flow rate of 3 L h^{-1}. When the regulation temperature was decreased to 600 °C (other conditions identical), the temperature increase was roughly 13 °C. At a regulation temperature of 570 °C, for the 80 mg sample, the temperature increase was 8 °C. When combustion was performed under 2% oxygen, the increase of the bed temperature was only 3 °C. The fact that the initial combustion rates were identical for masses larger that the critical mass (for given experimental conditions), shows that the temperature increase was only related to the combustion rate. This was due to the presence of inert material which maintained always the same volume of solid within the crucible. The effect of the difference of masses of inert material and CB from one experiment to another did not significantly affect the temperature increase. Therefore, when temperature measurement was impossible but when the experimental combustion rate was not varying (for the largest sample masses), the temperature increase was assumed to be also constant. These thermal effects were significant and had to be accounted for in the kinetic study.

Modelling and discussion

Intrinsic CB reactivity and oxygen transport govern CB combustion. A model of coupling between oxygen transport and reactivity is now presented to better understand to what extend transport of oxygen affects the process. Effect of sample containment will be discussed. A procedure to extract a reliable kinetic constant from thermogravimetric measurements will be proposed. The structure of the bed affects oxygen transport and evolves during combustion. The following study focuses on the initial material for which structure is better known.

Model of external oxygen transport

A model of oxygen transport from the oxidising flux to the surface of the bed of CB within the crucible of the thermobalance has already been presented [10]. Using the CFD package FLUENT, one estimates the oxygen mole fraction X_s at the bed surface at the beginning of different combustion runs under different experimental conditions. The main hypothesis is that the oxygen flux density entering the bed of CB is the same as the combustion rate per surface unit (steady state conditions). This flux is supposed to be uniformly distributed on the bed surface. Table 1 summarizes the X_s values, together with the experimental initial rates, for the different experimental situations. These values are not uniform along the bed radius, with the maximum close to the crucible walls. The maximum relative difference 23% is obtained for the higher combustion rate at a bed temperature measured at 670 °C, under 10% oxygen with 80 mg CB. This difference is depending on the combustion rate and is roughly 9 and 5% for the larger masses at 613 and 578 °C, respectively.

For an experiment without the presence of an inert material (50 mg CB, 600 °C, 10% oxygen), X_s was 0.076. The values of X_s are slightly dependent on the distance between the bed surface and the mouth of the crucible.

Model of internal oxygen transport and reaction

A one dimensional model of oxygen transport and reaction within the CB bed in a quasi-stationary regime leads to the following differential equation:

$$\frac{d^2X}{dz^2} - C_1 X^{\beta} = 0 \tag{3}$$

with

$$C_1 = \frac{fk\rho_{bed}}{D_{O_2} c M_C} \tag{4}$$

associated to the boundary conditions at the bed surface

$$z = 0, \quad X = X_s \tag{5}$$

Table 1 Experimental conditions and estimated parameters

Experiment number	m_0/mg	T_R/°C	T_{CB}/°C	X_{in}	X_s	f	k/s^{-1}	R_c/kg s^{-1}	D_{O_2}/m^2 s^{-1}	$(R_c)_{max}$/kg s^{-1}	η	R_c^{FB}/kg s^{-1}	R_c^{FB}/R_c
1	80	650	670	0.10	0.062	0.73	1.64×10^{-2}	1.25×10^{-8}	$(1.6 \pm 0.3) \times 10^{-5}$	1.14×10^{-7}	0.11	1.73×10^{-7}	13.8
2	50	650	670	0.10	0.062	0.73	1.64×10^{-2}	1.25×10^{-8}	$(1.6 \pm 0.3) \times 10^{-5}$	7.11×10^{-8}	0.18	1.08×10^{-7}	8.7
3	25	650	670	0.10	0.062	0.73	1.64×10^{-2}	1.25×10^{-8}	$(1.5 \pm 0.3) \times 10^{-5}$	3.56×10^{-8}	0.35	5.41×10^{-8}	4.3
4	20	650	670	0.10	0.062	0.73	1.64×10^{-2}	1.25×10^{-8}	$(1.6 \pm 0.3) \times 10^{-5}$	2.84×10^{-8}	0.44	4.33×10^{-8}	3.5
5	17.5[a]	650	670	0.10	0.062	0.73	1.64×10^{-2}	1.25×10^{-8}	$(1.6 \pm 0.3) \times 10^{-5}$	2.49×10^{-8}	0.50	3.79×10^{-8}	3.0
6	15	650		0.10	0.065	0.73	1.64×10^{-2}	1.12×10^{-8}		2.22×10^{-8}	0.50	3.25×10^{-8}	2.9
7	10	650		0.10	0.07	0.73	1.64×10^{-2}	6.2×10^{-9}		1.58×10^{-8}	0.39	2.16×10^{-8}	3.5
8	80	600	613	0.10	0.081	0.76	5.37×10^{-3}	6.2×10^{-9}	$(7 \pm 1) \times 10^{-6}$	4.71×10^{-8}	0.13	5.66×10^{-8}	9.1
9	50	600	613	0.10	0.081	0.76	5.37×10^{-3}	6.2×10^{-9}	$(7 \pm 1) \times 10^{-6}$	2.94×10^{-8}	0.21	3.54×10^{-8}	5.7
10	40	600	613	0.10	0.081	0.76	5.37×10^{-3}	6.2×10^{-9}	$(7 \pm 1) \times 10^{-6}$	3.35×10^{-8}	0.26	2.83×10^{-8}	4.6
11	30[a]	600	613	0.10	0.081	0.76	5.37×10^{-3}	6.2×10^{-9}	$(7 \pm 1) \times 10^{-6}$	1.77×10^{-8}	0.35	2.12×10^{-8}	3.4
12	27.5	600		0.10	0.084	0.76	5.37×10^{-3}	5.5×10^{-9}		1.66×10^{-8}	0.33	1.95×10^{-8}	3.5
13	25	600		0.10	0.087	0.76	5.37×10^{-3}	4.5×10^{-9}		1.56×10^{-8}	0.29	1.77×10^{-8}	3.9
14	10	600		0.10	0.094	0.76	5.37×10^{-3}	2.1×10^{-9}		6.70×10^{-9}	0.31	7.07×10^{-9}	3.4
15	80	570	578	0.10	0.088	0.80	2.51×10^{-3}	3.7×10^{-9}	$(4.6 \pm 0.7) \times 10^{-6}$	2.37×10^{-8}	0.16	2.64×10^{-8}	7.1
16	50	570	578	0.10	0.088	0.80	2.51×10^{-3}	3.7×10^{-9}	$(4.6 \pm 0.7) \times 10^{-6}$	1.48×10^{-8}	0.25	1.65×10^{-8}	4.5
17	40	570	578	0.10	0.088	0.80	2.51×10^{-3}	3.7×10^{-9}	$(4.6 \pm 0.7) \times 10^{-6}$	1.19×10^{-8}	0.31	1.32×10^{-8}	3.6
18	35[a]	570	578	0.10	0.088	0.80	2.51×10^{-3}	3.7×10^{-9}	$(4.6 \pm 0.7) \times 10^{-6}$	1.04×10^{-8}	0.36	1.16×10^{-8}	3.1
19	30	570		0.10	0.090	0.80	2.51×10^{-3}	3.25×10^{-9}		5.53×10^{-9}	0.59	6.07×10^{-9}	1.9
20	25	570		0.10	0.093	0.80	2.51×10^{-3}	2.2×10^{-9}		4.75×10^{-9}	0.46	5.06×10^{-9}	2.3
21	70	570	573	0.02	0.0174	0.83	2.24×10^{-3}	8.75×10^{-10}	$(6 \pm 1) \times 10^{-6}$	4.43×10^{-9}	0.20	5.01×10^{-9}	5.7
22	50	570	573	0.02	0.0174	0.83	2.24×10^{-3}	8.75×10^{-10}	$(6 \pm 1) \times 10^{-6}$	3.17×10^{-9}	0.28	3.58×10^{-9}	4.1
23	40	570	573	0.02	0.0174	0.83	2.24×10^{-3}	8.75×10^{-10}	$(6 \pm 1) \times 10^{-6}$	2.65×10^{-9}	0.33	3.01×10^{-9}	3.4
24	35[a]	570	573	0.02	0.0174	0.83	2.24×10^{-3}	8.75×10^{-10}	$(6 \pm 1) \times 10^{-6}$	2.21×10^{-9}	0.40	2.50×10^{-9}	2.9
25	28	570		0.02	0.0178	0.83	2.24×10^{-3}	7.85×10^{-10}		1.81×10^{-9}	0.43	2.00×10^{-9}	2.6

[a] Critical mass

at the interface between the sample bed and the inert material ($z = e$):

$$z = e, \quad \frac{dX}{dz} = 0 \tag{6}$$

Since the apparent kinetic constant k characterizes the whole spherule reactivity and is affected by diffusion within the spherule, the transport model ignores the porosity internal to spherules. Therefore, the equivalent diffusivity is only related to porosity external to spherules. The knowledge of k allows determining the effective oxygen diffusivity D_{O_2} at a given bed temperature. For every combustion run, the following procedure was used.

To estimate k at the bed temperature, Eq. 2 was used ($k = k^{FB}$). Assuming an arbitrary D_{O_2} value, a numerical resolution using Eqs. 3–5 allowed knowing X at any depth z. Then, Eq. 8 allowed calculating the CB initial combustion rate under the defined experimental conditions.

$$R_c = \int_0^e kS\rho_{bed}X^{\beta}dz \tag{7}$$

Temperature involved in calculations was that measured within the bed. If the calculated combustion rate was not equal to the experimental one, a new value of D_{O_2} was tested. This was repeated until agreement was obtained. For every experimental condition, the effective diffusivity D_{O_2} was calculated and reported in Table 1.

The main uncertainty about the estimated oxygen diffusivity comes from the kinetic input. Assuming 15% of uncertainty for the kinetic constant, one estimates diffusivity with a precision in the range 16–21%. Uncertainties are also given in Table 1.

The values of D_{O_2} are the same at a given temperature when the combustion rate is not affected by the sample mass. Surprisingly, they decrease with the sample mass (small masses) when the combustion rates decrease. This is probably due to the main hypothesis of the model assuming a one dimensional transport of oxygen. This hypothesis is very questionable for small samples for which the bed height is less than 1 mm, i.e., less than 1/7 of the crucible radius. The very small mass comprising only few particles along the bed thickness, the pile may become very irregular. It was, however, possible to obtain repeatable measurements by paying a lot of attention to crucible filling. The main problem lies in the fact that concentration gradients appear along the radial coordinate when the bed thickness is small compared to the radius. In that case, a one dimensional model is not appropriate. For that reason, the diffusion coefficients obtained from combustion of larger masses are retained.

Oxygen diffusivities range from 1.6×10^{-5} m^2 s^{-1} at 670 °C to 4.6×10^{-6} m^2 s^{-1} at 578 °C. A global decrease of the diffusivity with temperature is pointed out.

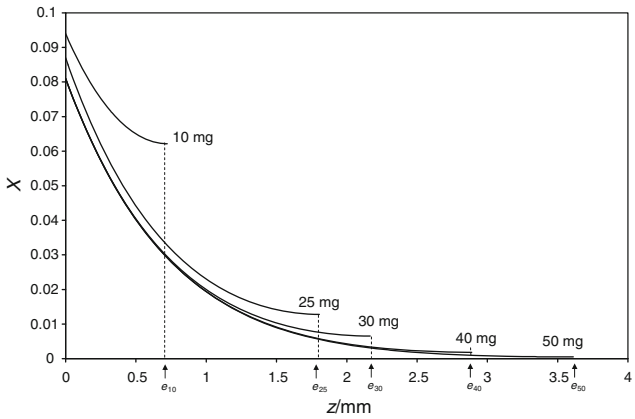

Fig. 10 Oxygen molar fraction at any depth at the beginning of the combustion of different initial masses of CB, at 600 °C (regulation temperature) under 10% oxygen. $D_{O_2} = 7 \times 10^{-6}$m^{2}s^{-1}. e_{10}, e_{25}, e_{30}, e_{40} and e_{50} are the thicknesses of the bed of CB corresponding to 10, 25, 30, 40 and 50 mg, respectively

Figure 10 exhibits the oxygen mole fraction profiles obtained for a regulation temperature of 600 °C and 10% O_2, using $D_{O_2} = 7 \times 10^{-6}$ m^2 s^{-1}, for the different sample masses. For masses smaller than 30 mg, considering a bed temperature of 613 °C, the oxygen molar fraction never falls to zero within the bed. Above 30 mg, the oxygen molar fraction falls close to zero before the bottom of the CB bed.

The bed of CB exhibits a very high total porosity (0.82). Aggregates themselves are very porous. This makes reasonable to think that Fickian oxygen diffusion prevails within the CB bed, around the spherules. The Fickian diffusivity of oxygen within a porous bed writes

$$D_{O_2} = 1.78 \times 10^{-5}\left(\frac{T}{273}\right)^{1.75}\frac{\varepsilon}{\tau} \tag{8}$$

with τ the bed tortuosity and ε the total porosity. The value of tortuosity ranges between 2 and 10 [18]. Since the considered porous medium comprises three porosity levels, the maximum value of 10 is assumed in this model.

At 613 °C, the Fickian diffusion coefficient is 1.1×10^{-5} m^2 s^{-1}. This value is roughly 1.6 times the diffusion coefficient obtained from thermogravimetric experiments. This ratio is 0.8 at 670 °C and 2.3 at 578 °C. This means that Fickian diffusivity may be a good approximate to model oxygen transport within the bed. The fact that the determined diffusivity is generally found smaller than the Fickian one is certainly related to some diffusional limitations within aggregates, between spherules. A tortuosity selected at 10 allows to minimize the shift between the diffusivity calculated from thermogravimetric experiments and the Fickian diffusivity.

Effectiveness factor of the bed of CB

The combustion rate of the bed is related to the oxygen mole fraction profile along the bed thickness. For a given value for X_s, the combustion rate would be at a maximum for a uniform oxygen mole fraction within the bed equal to the surface value. Therefore, the maximum combustion rate writes

$$(R_C)_{max} = kS\rho_{bed}X_S^{\beta}e = m_0kX_S^{\beta} \quad (9)$$

The effectiveness factor η of the bed is defined by

$$\eta = \frac{R_C}{(R_C)_{max}} \quad (10)$$

The values of η for the different experimental conditions are calculated at the beginning of the combustion and are given in Table 1. As expected, for given temperature and inlet oxygen content, η decreases with the initial sample mass. Under high rate conditions (670 °C and 10% oxygen), a very weak efficiency of 0.11 is obtained for 80 mg of CB. On the other hand, a maximum value of 0.5 is obtained for 17.5 mg of CB. For a given sample mass, the effectiveness factor increases when the combustion rate decreases. The effectiveness factor ranges between 0.11 and 0.6, showing poor bed efficiency obtained during thermogravimetric combustion. In a fixed bed, since there is no oxygen concentration gradient along the bed thickness, the effectiveness factor of the bed is 1.

The combustion rate obtained with the fixed bed is the upper limit of the thermogravimetric rate which would be obtained without any external ($X_s = X_{in}$) and internal (effectiveness factor equal to 1) diffusional limitations. For given temperature and oxygen inlet mass fraction, the ratio between the combustion rate obtained with the fixed bed and the one obtained by thermogravimetry writes

$$\frac{R_C^{FB}}{R_C} = \frac{R_C^{FB}}{\eta(R_C)_{max}} \quad (11)$$

Since $(R_C)_{max}$ is proportional to the inlet oxygen mole fraction

$$(R_C)_{max} = \left(\frac{X_S}{(X_{in})}\right)^{\beta}\left((R_C)_{max}\right)_{in} \quad (12)$$

with $((R_C)_{max})_{in}$ the combustion rate of carbon if the oxygen mole fraction was uniformly X_{in} within the bed. This would be the thermogravimetric rate without any diffusional limitations. Then, since diffusional limitations are not at work in the fixed bed,

$$R_C^{FB} = \left((R_C)_{max}\right)_{in} \quad (13)$$

Then,

$$\frac{R_C^{FB}}{R_C} = \left(\frac{X_{in}}{X_S}\right)^{\beta}\frac{1}{\eta} \quad (14)$$

This ratio is directly related to external diffusional limitations responsible for the value of $\left(\frac{X_{in}}{X_S}\right)^{\beta}$, and to internal limitations contained in the effectiveness factor η. This ratio is calculated for every experimental situation and is given in Table 1.

This ratio increases when η decreases and when X_s is far from X_{in}. This ratio ranges from 2 to 14 with the higher values for a high temperature and a large sample mass.

Extraction of a kinetic constant from thermogravimetry

The combustion process in thermogravimetry has been characterized by a kinetic parameter k and a transport parameter D_{O_2}, which both depend on temperature. A thermobalance is currently used to determine the kinetic parameter.

A very precise determination of the kinetic parameter k from a thermogravimetric experiment necessitates, a priori, to model oxygen transport coupled to reaction. Very often, more simple determinations, with no transport model or a simplified one, are performed, giving approximate values of the kinetic parameter. According to the simplifications used in the calculation procedure, the experimental conditions can be adapted to optimize the determination of k.

When a thermobalance is used, the main problem is to know the sample temperature during reaction. This temperature is impossible to measure and difficult to estimate precisely by modelling. For that reason, the regulation temperature of the thermobalance is often considered as the sample temperature.

Let us define four procedures allowing k determination.

1. *Procedure 1*. The sample temperature is known. Internal oxygen transport within the bed is modelled, coupled with reaction. The Fick diffusivity of oxygen is used. The external oxygen transport is also considered, using a CFD code, as described previously. This procedure is the most sophisticated one. The only simplification is to impose a Fickian diffusivity of oxygen within the porous medium. The kinetic constant obtained with this procedure is noted k_1. This constant is compared to the kinetic constant obtained with the fixed-bed reactor, noted k^{FB} and calculated with Eq. 2 at the sample temperature. Comparison is performed through the ratio $R_1 = \frac{k^{FB}}{k_1}$ calculated at the sample temperature. The constant k_1 and the ratio R_1 are given in Table 2 for each experimental condition, when the sample temperature is known.

2. *Procedure 2*. The sample temperature is not known so that the regulation temperature is assumed to be the sample temperature. This means that the sample temperature may be underestimated. Internal oxygen transport is modelled, but not external one. Then the oxygen molar fraction at the surface of the bed is assumed to be X_{in}. The kinetic

Table 2 Calculated values of the kinetic constants according to the determination procedures 1, 2, 3 and 4, respectively

Experiment number	m_0/mg	T_R/°C	T_{CB}/°C	X_{in}	X_s	k^{FB}/s^{-1} at T_{CB}	k^{FB}/s^{-1} at T_R	k_1/s^{-1}	R_1	k_2/s^{-1}	R_2	k_3/s^{-1}	R_3	k_4/s^{-1}	R_4
1	80	650	670	0.10	0.062	1.64×10^{-2}	1.13×10^{-2}	2.05×10^{-2}	0.8	1.80×10^{-3}	6.3	8.30×10^{-3}	1.4	1.19×10^{-3}	9.5
2	50	650	670	0.10	0.062	1.64×10^{-2}	1.13×10^{-2}	2.05×10^{-2}	0.8	2.88×10^{-3}	3.9	8.14×10^{-3}	1.4	1.90×10^{-3}	6.0
3	25	650	670	0.10	0.062	1.64×10^{-2}	1.13×10^{-2}	1.95×10^{-2}	0.8	5.77×10^{-3}	2.0	8.28×10^{-3}	1.4	3.79×10^{-3}	3.0
4	20	650	670	0.10	0.062	1.64×10^{-2}	1.13×10^{-2}	1.95×10^{-2}	0.8	7.21×10^{-3}	1.6	8.75×10^{-3}	1.3	4.74×10^{-3}	2.4
5	17.5[a]	650	670	0.10	0.062	1.64×10^{-2}	1.13×10^{-2}	1.96×10^{-2}	0.8	8.24×10^{-3}	1.4	9.20×10^{-3}	1.2	5.42×10^{-3}	2.1
6	15	650		0.10	0.065		1.13×10^{-2}			8.29×10^{-3}	1.4	8.39×10^{-3}	1.3	5.66×10^{-3}	2.0
7	10	650		0.10	0.07		1.13×10^{-2}			6.44×10^{-3}	1.8	5.40×10^{-3}	2.1	4.70×10^{-3}	2.4
8	80	600	613	0.10	0.081	5.37×10^{-3}	4.07×10^{-3}	3.21×10^{-3}	1.7	7.06×10^{-4}	5.8	2.17×10^{-3}	1.9	5.88×10^{-4}	6.9
9	50	600	613	0.10	0.081	5.37×10^{-3}	4.07×10^{-3}	3.18×10^{-3}	1.7	1.13×10^{-3}	3.6	2.22×10^{-3}	1.8	9.41×10^{-4}	4.3
10	40	600	613	0.10	0.081	5.37×10^{-3}	4.07×10^{-3}	3.24×10^{-3}	1.7	1.41×10^{-3}	2.9	2.30×10^{-3}	1.8	1.18×10^{-3}	3.5
11	30[a]	600	613	0.10	0.081	5.37×10^{-3}	4.07×10^{-3}	3.46×10^{-3}	1.6	1.88×10^{-3}	2.2	2.55×10^{-3}	1.6	1.57×10^{-3}	2.6
12	27.5	600		0.10	0.084		4.07×10^{-3}			1.78×10^{-3}	2.3	2.24×10^{-3}	1.8	1.52×10^{-3}	2.7
13	25	600		0.10	0.087		4.07×10^{-3}			1.55×10^{-3}	2.6	1.81×10^{-3}	2.2	1.37×10^{-3}	3.0
14	10	600		0.10	0.094		4.07×10^{-3}			1.68×10^{-3}	2.4	1.67×10^{-3}	2.4	1.59×10^{-3}	2.6
15	80	570	578	0.10	0.088	2.51×10^{-3}	2.11×10^{-3}	1.06×10^{-3}	2.4	3.91×10^{-4}	5.4	8.50×10^{-4}	2.5	3.51×10^{-4}	6.0
16	50	570	578	0.10	0.088	2.51×10^{-3}	2.11×10^{-3}	1.15×10^{-3}	2.2	6.26×10^{-4}	3.4	9.60×10^{-4}	2.2	5.61×10^{-4}	3.8
17	40	570	578	0.10	0.088	2.51×10^{-3}	2.11×10^{-3}	1.26×10^{-3}	2.0	7.82×10^{-4}	2.7	1.06×10^{-3}	2.0	7.02×10^{-4}	3.0
18	35[a]	570	578	0.10	0.088	2.51×10^{-3}	2.11×10^{-3}	1.35×10^{-3}	1.9	8.94×10^{-4}	2.4	1.15×10^{-3}	1.8	8.02×10^{-4}	2.6
19	30	570		0.10	0.090		2.11×10^{-3}			9.03×10^{-4}	2.3	1.07×10^{-3}	2.0	8.22×10^{-4}	2.6
20	25	570		0.10	0.093		2.11×10^{-3}			7.12×10^{-4}	3.0	7.70×10^{-4}	2.7	6.68×10^{-4}	3.2
21	70	570	573	0.02	0.0174	2.24×10^{-3}	2.11×10^{-3}	1.31×10^{-3}	1.7	4.42×10^{-4}	4.8	1.05×10^{-3}	2.0	3.91×10^{-4}	5.4
22	50	570	573	0.02	0.0174	2.24×10^{-3}	2.11×10^{-3}	1.35×10^{-3}	1.7	6.19×10^{-4}	3.4	1.11×10^{-3}	1.9	5.47×10^{-4}	3.9
23	42	570	573	0.02	0.0174	2.24×10^{-3}	2.11×10^{-3}	1.43×10^{-3}	1.6	7.38×10^{-4}	2.9	1.18×10^{-3}	1.8	6.51×10^{-4}	3.2
24	35[a]	570	573	0.02	0.0174	2.24×10^{-3}	2.11×10^{-3}	1.50×10^{-3}	1.5	8.86×10^{-4}	2.4	1.27×10^{-3}	1.7	7.82×10^{-4}	2.7
25	28	570		0.02	0.0178		2.11×10^{-3}			9.70×10^{-4}	2.2	1.25×10^{-3}	1.7	8.77×10^{-4}	2.4

[a] Critical mass

Table 3 Summary of the hypotheses used for determination of k_1, k_2, k_3 and k_4

	Internal limitations	External limitations	Temperature
Procedure 1	Yes	Yes	T_{CB}
Procedure 2	No	Yes	T_R
Procedure 3	Yes	No	T_R
Procedure 4	No	No	T_R

Summary of notation

constant obtained with this procedure is noted k_2 and is compared to k^{FB} calculated at the regulation temperature (Eq. 2) using the ratio $R_2 = \frac{k^{FB}}{k_2}$ (see Table 2).

3. *Procedure 3*. Compared to procedure 2, the only difference is that only external oxygen transport is modelled using the CFD code. The oxygen fraction of oxygen is then assumed to be uniform within the bed with its value X_s calculated at the surface. The combustion rate of CB is then written

$$R_C = k_3 m_0 X_s^{\beta} \quad (15)$$

The calculated kinetic constant obtained with this procedure is noted k_3 and is compared to k^{FB} calculated at the regulation temperature (Eq. 2) using the ratio $R_3 = \frac{k^{FB}}{k_3}$ (see Table 2).

4. *Procedure 4*. This last procedure is the simplest one. The sample temperature is not known. Sample is assumed to be at the regulation temperature. Oxygen transport, either internal or external, is not modelled. Then, the oxygen molar fraction is assumed to be uniform within the bed with its value X_{in} at the inlet of the thermobalance. The combustion rate of CB is then written

$$R_C = k_4 m_0 X^{\beta} \quad (16)$$

The calculated kinetic constant obtained with this procedure is noted k_4 and is compared to k^{FB} calculated at the regulation temperature (Eq. 2) using the ratio $R_4 = \frac{k^{FB}}{k_4}$ (see Table 2).

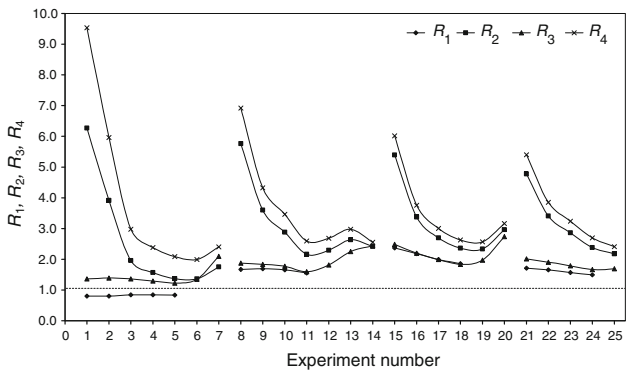

Fig. 11 Ratios R_1 to R_4 for the different experimental conditions

Table 3 summarizes the hypotheses used in the different procedures and the notations for the different constants and ratios.

The different ratios calculated for the different experiments, according to the four procedures, are plotted on Fig. 11.

The comparison of the kinetic constants returned by the different models to the constant obtained with the fixed bed is based on the fact that this latter one is expected to be intrinsic. Then, if the sample temperature is known and if oxygen mass transfer limitations are correctly accounted for, the ratio $R = \frac{k^{FB}}{k}$ should be 1.

Ratios obtained with procedure 1 are between 1 and 2, whatever the experimental conditions. This means that, whatever the sample mass, diffusional limitations are correctly predicted by the model. The shift between the two constants k_1 and k^{FB} is mainly due to the choice of the Fickian diffusivity of oxygen. The modelling of internal transport of oxygen may be optimized by changing this diffusivity, necessitating a fitting procedure to determine the best diffusion parameter.

Ratios R_2 obtained by procedure 2 which accounts for internal diffusional limitations and ignores external ones, are very close to ratios obtained with procedure 1. For smaller samples masses, the ratio R_2 tends to slightly decrease. This could be due to the questionable validity of a one dimensional model for internal oxygen transport in case of a very thin sample bed. Then, the use of the regulation temperature and ignorance of external transport limitations seem to be possible approximations when the sample mass remains bigger than 30 mg.

Ratios R_3 and R_4 which both ignore internal transport limitations are far from 1, especially for the biggest sample masses. This means that it appears mandatory to account for internal oxygen transport limitations, whatever the sample mass but especially for sample masses bigger than 30 mg. To account for external diffusional limitations does not significantly improve the estimation of the kinetic constant. To account for internal diffusional limitations makes the big difference between R_1, R_2 on one side and R_3, R_4 on the other side.

Conclusions

The experimental and theoretical study of CB combustion using thermogravimetry has shown the importance of limitations to oxygen transport within the sample bed in the combustion control. When a kinetic constant is extracted from a thermogravimetric experiment, the experimental procedure and the procedure used to extract the constant must be optimized. The best procedure, kept simple, seems to be:

- to use a sample mass between 30 and 50 mg, not to high to limit thermal effects and not to small to obtain a thick enough sample bed for model purposes,
- to minimize external oxygen transport limitations and thermal effects by use of an inert material to make the surface of the sample close to the mouth of the crucible,
- to model internal oxygen transport, using the Fickian diffusivity of oxygen in a first approach,
- to neglect external oxygen diffusion limitations,
- to assume that the sample temperature is the regulation temperature,
- to investigate different experimental conditions (varying initial sample masses for example) to validate the constant determination,
- to improve, if necessary, the constant determination by optimizing the value of oxygen diffusivity to model internal oxygen transport.

References

1. Šestak J, Berggren G. Study of the kinetics of the mechanism of solid-state reactions at increasing temperatures. Thermochim Acta. 1971;3:1–12.
2. Šatava V. Fundamental principles of kinetic data evaluation from thermal analysis curves. J Thermal Anal. 1973;5:217–26.
3. Ceipidor UB, Bucci R, Magri AD. Using thermoanalytical data. Part 2. The dependence of kinetic data available from thermogravimetry on sample and instrument parameters: a method for calculating 'true' kinetic parameters. Thermochim Acta. 1990; 161:37–49.
4. Kalogirou M, Samaras Z. Soot oxidation kinetics from TG experiments. J Thermal Anal Calorim. 2009;98:215–24.
5. Kalogirou M, Samaras Z. Soot oxidation kinetics from TG experiments, Can they be used reliably in diesel particulate filter modelling tools? J Thermal Anal Calorim. 2010;99:1005–10.
6. Czarnecki J, Šestak J. Practical thermogravimetry. J Thermal Anal Calorim. 2000;60:759–78.
7. Ollero P, Serrera A, Arjona R, Alcantarilla S. Diffusional effects in TGA gasification experiments for kinetic determination. Fuel. 2002;81:1989–2000.
8. Gómez-Barea A, Ollero P, Arjona R. Reaction-diffusion model of TGA gasification experiments for estimating diffusional effects. Fuel. 2005;84:1695–704.
9. Marcuccilli F, Gilot P, Stanmore B, Prado G. Experimental and theoretical study of diesel soot reactivity. Twenty-Fifth Symposium (International) on Combustion, The Combustion Institute, Pittsburgh; 1994. pp. 619–26.
10. Stanmore BR, Gilot P. The influence of sample containment on the thermogravimetric measurement of carbon black reactivity. Thermochim Acta. 1995;261:151–64.
11. Gilot P, Brillard A, Stanmore BR. Geometric effects on mass transfer during thermogravimetric analysis: application to reactivity of diesel soot. Combust Flame. 1995;102:471–80.
12. Ishiguro T, Suzuki N, Fujitani Y, Morimoto H. Microstructural changes of diesel soot during oxidation. Combust Flame. 1991;85:1–6.
13. Neeft JPA, Nijhuis TX, Smakman E, Makkee M, Moulijn J. Kinetics of the oxidation of diesel soot. Fuel. 1997;67:1129–36.
14. Yezerets A, Currier NW, Kim DH, Eadler HA, Epling WS, Peden CHF. Differential kinetic analysis of diesel particulate matter (soot) oxidation by oxygen using a step–response technique. Appl Catal B. 2005;61:120–9.
15. Walker PL Jr, Taylor RL, Ranish JM. An update on the carbon–oxygen reaction. Carbon. 1991;29:411–21.
16. Nguyen Huu Nhon Y, Mohamed Magan H, Petit C. Catalytic diesel particulate filter: evaluation of parameters for laboratory studies. Appl Catal B. 2004;49:127–33.
17. Jung H, Kittelson DB, Zachariah MR. Kinetics and visualization of soot oxidation using transmission electron microscopy. Combust Flame. 2004;136:445–56.
18. Schweich D. Proc. Ecole d'été "Transfert en milieu poreux", vol. 2, Carcans-Maubuisson; 1985.